Total Scattering Cross Section and Spin Motion of Low Energy Electrons Passing through a Ferromagnet

D. Oberli, R. Burgermeister, S. Riesen, W. Weber, and H. C. Siegmann
Laboratorium für Festkörperphysik, ETH Zürich, CH-8093 Zürich, Switzerland
(Received 10 June 1998)

It is shown that the spin asymmetry of the elastic transmission of electrons through ferromagnetic films can approach unity. The polycrystalline Co films are a few nanometers thick and saturated with the magnetization $\vec{M}$ in the plane. The contribution of spin-productive scattering events is below 5%. If the electron spin at incidence is chosen to be perpendicular to $\vec{M}$, it rotates into the direction of $\vec{M}$ and also precesses around it. [S0031-9007(98)07521-8]

PACS numbers: 73.50.Yg, 79.20.Kz

The application of polarized electron beams to the study of magnetism took its beginning when the first spin-polarized electrons were obtained by photoemission from magnetic materials [1]. The most obvious way of looking at photoemission of electrons theoretically is to assume that the fast photoelectron does not interact appreciably with the other electrons in the metal so that the photoemission experiment often is thought of as measuring the energy spectrum of its own hole state left behind. This theory of renormalized one-electron states has been discussed in the present context by Anderson [2], Doniach [3], Gutzwiler [4], and many others [5]. However, it could never explain the fact that no negative spin polarization is detected in photoemission from states near the Fermi energy E_F in Co [6,7]. This and many other features observed in emission of low energy electrons from transition metals are now understood by considering the scattering of the excited electron on the partially filled d states of *all* of the atoms encountered in transport through the transition metal [8]. To study this important phenomenon more thoroughly, we have measured the total scattering cross section as a function of electron energy. In contrast to numerous earlier investigations [9], we have observed very large transmission asymmetries A of up to 80% with an electron beam passing through a thin ferromagnet depending on whether its spin is parallel or antiparallel to the magnetization $\vec{M}$. Furthermore, when the spin polarization vector $\vec{P}_0$ of the incident electron beam is chosen to be perpendicular to $\vec{M}$, then it rotates into the direction of $\vec{M}$ and simultaneously also precesses around $\vec{M}$. There is a complete analogy to the magneto-optic phenomena observed when a light beam passes through ferromagnetic material. But, even when measured on the length scale of the penetration depth, the magneto-"optic" effects observed with electron beams are at least 1 order of magnitude larger as compared to those observed with light beams. This arises because the electron beam couples directly to the magnetization, while the coupling of the light beam must be mediated by the spin-orbit interaction. The observations presented here have a number of immediate important implications. For instance, the scattering cross section governs the nonequilibrium magnetization dynamics which is presently at the forefront of fundamental research in magnetism [10–13]. Furthermore, experiments of the type described here might help to improve the performance of spin filters, spin transistors, and spin tunneling, and may also lead to magnetic imaging in transmission electron microscopy.

The experiment is sketched in the upper part of Fig. 1. We have prepared a spin-modulated electron beam with a GaAs-type photocathode. By switching from right- to left-circularly polarized light for excitation of the source, we can invert the vector $\vec{P}_0$ of the spin polarization. By applying a combination of electric and magnetic fields to

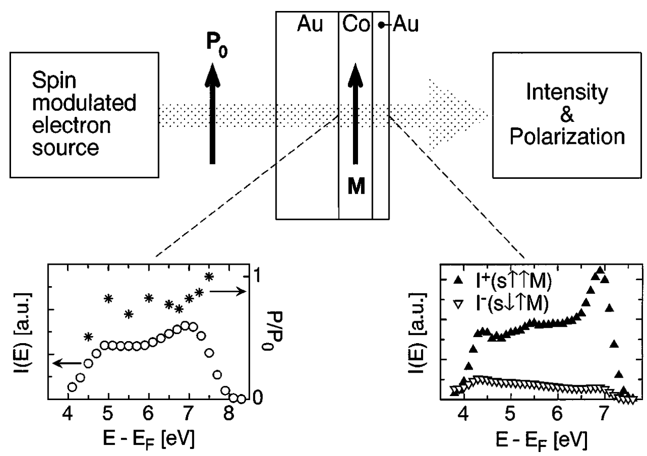

FIG. 1. The upper part shows the principle of the experiment consisting of a spin-modulated electron source of the GaAs type, a Au/Co/Au trilayer in which the ferromagnetic polycrystalline hcp Co film is magnetized remanently in the plane, and a detection system in which the intensity I and degree of spin polarization P perpendicular to the axis of the electron beam are measured for the electrons transmitted by the trilayer. The lower part shows on the left the energy distribution curve $I(E)$ and the degree of relative polarization P/P_0 after the electron beam has traversed the supporting Au layer alone. P_0 is the degree of spin polarization delivered by the source. In the lower part on the right, the intensity distribution curves $I^+(E)$ and $I^-(E)$ are shown for a Co film of 4 nm thickness and its 2 nm thick Au capping added. $I^+(E)$ is valid for spin parallel to the magnetization $\vec{M}$, and $I^-(E)$ for spin antiparallel to $\vec{M}$.

 0031-9007/98/81(19)/4228(4)$15.00

the electron beam, we can also rotate $\vec{P}_0$ into any desired direction in space. We can produce an unpolarized electron beam as well by applying linearly polarized light.

The spin-polarized electron beam impinges along the surface normal onto a trilayer consisting of a supporting Au film 20 nm thick, a ferromagnetic Co layer of varying thickness ranging from 1–6 nm, and a capping Au layer of 2 nm thickness to prevent corrosion. In this geometry spin-orbit coupling cannot produce any spin dependence of the transmission.

The trilayer is made in a separate chamber on a substrate consisting of a film of nitrocellulose supported by a Si wafer with a number of 0.5 mm wide apertures. The Au layer of 20 nm thickness is deposited on top of the nitrocellulose by evaporation of Au from a heated Mo crucible. On top of this layer, polycrystalline films of hcp Co are deposited by electron bombardment of a 99.998% pure Co rod. Their thickness (as measured by a calibrated quartz microbalance) ranges from 1–6 nm. The Co films are capped with a protecting Au layer of 2 nm thickness. The first set of hysteresis loops is measured right after deposition by *in situ* Kerr magnetometry. The in-plane hysteresis loops are square and exhibit full magnetic remanence. After the magnetic tests are completed, the whole sample is let to air. The nitrocellulose on the apertures is removed in a solution of pentyl acetate. The sample is then introduced through a load-lock system into the chamber with the GaAs electron source where the measurements are done. There, the sample is first exposed to mild sputtering designed to get rid of the contaminants acquired in the process of letting it to air and dissolving the nitrocellulose. Further sputtering through the apertures thins the supporting Au layer until electrons of a primary energy of ~6 eV above E_F are transmitted at an attenuation of 10^{-5}–10^{-6}. The final thickness of the supporting Au layer is estimated at ~18 nm. The Kerr hysteresis loops taken later show no difference to the loops obtained just after deposition of the samples.

In the actual measurements, the Co films are remanently magnetized in the plane by applying a positive or negative magnetic field pulse. The electrons emerging from the Au/Co/Au multilayer are energy analyzed by a retarding field, and subsequently accelerated to an energy of 100 keV to determine the components of the spin polarization vector perpendicular to the axis of the electron beam via Mott scattering.

In the lower part of Fig. 1 we show data observed with an incident electron beam of about 7 eV energy and $\vec{P}_0$ perpendicular to the electron beam. The inset on the left shows intensity and polarization as a function of energy without the Co film in order to illustrate what kind of an electron beam actually enters the ferromagnet. In the energy distribution curve $I(E)$ one distinguishes still an elastic peak at 7 eV, but secondary electrons have of course also been produced in Au at lower energies. However, the spin polarization of the elastic electrons is not altered on passing through the Au film. Yet the secondaries having suffered collisions with valence electrons in Au have a lowered polarization that decreases with decreasing energy due to the increasing admixture of unpolarized electrons excited from the conduction bands of Au.

The inset at the right shows data when a Co film of thickness $y = 4$ nm with its Au capping is added. One observes two different energy distribution curves of the emerging electron beam. I^+ is valid for $\vec{P}_0$ parallel and I^- for $\vec{P}_0$ antiparallel to $\vec{M}$, where the direction of $\vec{M}$ is defined by the direction of the majority spins. The elastic part of the beam displays a huge spin asymmetry $A = (I^+ - I^-)/(I^+ + I^-)$ for a pure spin state. On the other hand, the inelastic part of the electron spectrum exhibits lower A. This is partly due to the lower polarization of the inelastic electrons generated in the supporting Au layer. In the following, we focus on the elastic part of the spectrum which we can separate by applying a retarding field.

The most important condition for observing the large A is that the trilayer must have absolutely no holes. This is evident from Fig. 2, where the relative intensity transmitted through the Au/Co/Au is shown vs the energy E of the incident electron beam. The attenuation increases by 3 orders of magnitude when E increases from 6 eV above E_F to 16 eV. If there is the tiniest hole, the main part of the elastic signal observed at the back side of the trilayer is caused by electrons that have passed through the hole. We suspect that this is the reason why much smaller A values were reported in Ref. [14] at higher electron energies. The steep increase of the attenuation with increasing E is in reasonable agreement with the energy dependence of the electron mean free path in Au [15].

We now consider the attenuation of the elastic electron beam in the Co film of thickness y for each spin direction separately. With the incident current I_0 the transmitted current is $I = I_0 e^{-\sigma y}$. The absorption coefficient σ depends on the angle ϕ between $\vec{P}_0$ and $\vec{M}$; the largest value σ^- occurs with $\phi = \pi$ and the smallest

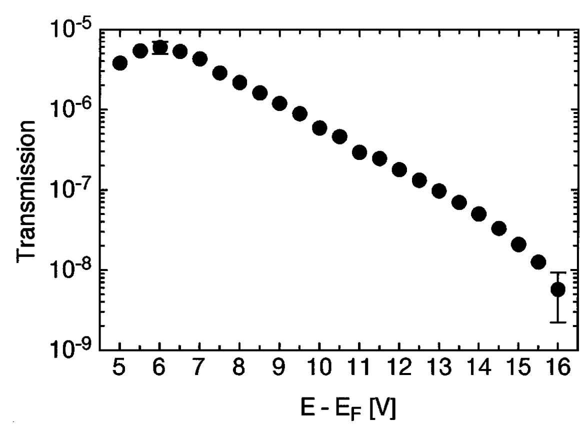

FIG. 2. The attenuation of the elastic electrons after penetration of the trilayer vs the energy above the Fermi energy E_F.

σ^+ with $\phi = 0$. With $\Delta\sigma = \sigma^- - \sigma^+$, we have $A = [\exp(\Delta\sigma y) - 1]/[\exp(\Delta\sigma y) + 1]$. One obtains

$$\Delta\sigma = \frac{1}{y}\ln\left(\frac{I^+}{I^-}\right). \quad (1)$$

Figure 3 shows a number of data obtained with various samples. To interpret this further, we assume that all of the spin-dependent scattering is scattering on the d shell, and that the strength of the scattering is proportional to the number of holes in that shell. The number of holes in the d shell is not *a priori* known for atoms in a metal. However, with the ferromagnetic metals, one knows the spin part of the saturation magnetization which is the difference in the occupancy of the d shell between majority- and minority-spin electrons known as the number of Bohr magnetons, n_B, per atom. With the present electron energies several eV above E_F, all of the d holes are available for scattering. This yields $\Delta\sigma = n_B\sigma_d$, where σ_d is the absorption coefficient for one unoccupied state in the $3d$ shell in Co. This approach is well supported by a number of quite different experiments [16].

With hcp Co, the density of atoms is $N = 8.6 \times 10^{28}$ atoms/m^3 and $n_B = 1.7$ Bohr magnetons. Hence, one obtains the following for the total scattering cross section:

$$Q = \frac{1}{Nn_B y}\ln\left(\frac{I^+}{I^-}\right). \quad (2)$$

The lower part of Fig. 3 shows Q calculated from the average of $\Delta\sigma$. The order of magnitude of Q reflects the fact that the d shell is comparatively little extended in space. For the interpretation one must be aware that Q is the sum of all scattering on the d shell, elastic and inelastic. Gokhale and Mills [17] have shown on the example of a single crystalline Fe film that effects of elastic scattering plus crystal diffraction and channeling can lead to sizable contributions to the spin-dependent transmission. However, these contributions favor both majority-spin and minority-spin transmission depending on the energy. Furthermore, they are generally not as large as observed here and also tend to increase on increasing the electron energy above 10 eV. Furthermore, crystal diffraction must cancel out for truly polycrystalline samples. We believe therefore that the main contribution to the total scattering cross section Q in Fig. 3 obtained from the average of $\Delta\sigma$ on all polycrystalline samples reflects predominantly the inelastic scattering on the d shell.

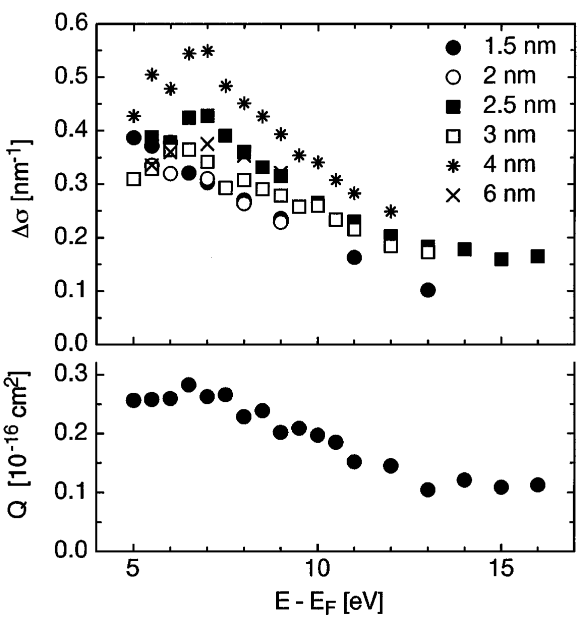

FIG. 3. Difference in the absorption coefficient $\Delta\sigma$ for majority- and minority-spin electrons vs electron energy for six samples each with a different Co thickness. The lower graph shows the average total scattering cross section Q for one hole in the $3d$ shell of Co.

To analyze the spin-selective scattering in ferromagnets in more depth, one must ask the question of what happens after the minority-spin electron has scattered into a hole of the d shell forming one of the $3d^{n+1}$ multiplet states. It has been argued [18] that the excess energy is dissipated by reemitting a majority-spin electron which, however, has lost at least the energy of the Stoner gap δ. In total, this process, called a Stoner excitation, would have made out of a minority spin in the primary electron beam a majority spin with a small energy loss δ. Such Stoner excitations have been detected experimentally [19,20]. We can test how important these excitations are in the spin-polarized transmission by making use of the theorem that a polarizing spin filter must be equal to an analyzing spin filter in the absence of spin-productive scattering events such as Stoner excitations [21]. The change in the majority-spin current is $dI^+ = -\sigma^+ I^+ dy - \alpha dI^-$, and in the minority-spin current $dI^- = -\sigma^- I^- dy$, where α is a constant. The fraction of minority-spin electrons that has undergone a spin flip in a Stoner excitation but is still detected in the elastic channel because δ is small, typically a fraction of an eV, is given by $r = \alpha/(1 - \alpha + \sigma^+/\sigma^-)$. The polarization P of an unpolarized electron beam passing through the ferromagnet will be

$$P = A + P^*(A, r, y), \quad (3)$$

while it is $P = A$ for $r = 0$. Experimentally, the comparison of P and A shows that the contribution of Stoner excitations r is below 5% and thus of minor importance in spin-dependent transmission.

We now consider the situation in which $\vec{P}_0$ is perpendicular to $\vec{M}$. In this case the spin part of the incident electron wave function can be described as a coherent superposition of a majority-spin ($\vec{s}$ parallel to $\vec{M}$) and a minority-spin ($\vec{s}$ antiparallel to $\vec{M}$) wave function with equal amplitudes: $\psi_0 = \frac{1}{\sqrt{2}}[\binom{1}{0} + \binom{0}{1}]$. Because of spin-dependent absorption, the amplitude of the two wave functions becomes different on passing the ferromagnet.

A phase difference ϵ develops as well. This yields the following for the wave function ψ of the electrons leaving the ferromagnet:

$$\psi = \frac{1}{\sqrt{2}} \left[\sqrt{1 + A} \begin{pmatrix} 1 \\ 0 \end{pmatrix} e^{-i\epsilon/2} + \sqrt{1 - A} \begin{pmatrix} 0 \\ 1 \end{pmatrix} e^{+i\epsilon/2} \right].$$

The spin polarization vector $\vec{P}$ of the transmitted electrons is determined by the expectation values of the Pauli matrices. (Note that the x axis is parallel to $\vec{P}_0$, the y axis is parallel to the electron beam, and the z axis is parallel to $\vec{M}$.) This yields

$$\vec{P} = \begin{pmatrix} P_0\sqrt{1 - A^2}\cos(\epsilon) \\ P_0\sqrt{1 - A^2}\sin(\epsilon) \\ A \end{pmatrix}, \tag{4}$$

and corresponds to two types of motion of the spin polarization vector, namely, a rotation by an angle of ϕ into the direction of $\vec{M}$ and a precession by an angle of ϵ around $\vec{M}$.

The rotation takes place in the plane spanned by $\vec{P}$ and $\vec{M}$. This rotation is due to absorption in the ferromagnetic film, as discussed above, where the minority-spin wave function is more strongly attenuated than the majority-spin wave function. The angle ϕ of the rotation is given by

$$\tan\phi = \frac{A}{P_0\sqrt{1 - A^2}}. \tag{5}$$

The direct measurement of ϕ confirms Eq. (5). For example, for a Co film with $A = 0.3$, ϕ for a pure spin state is $\approx 17°$.

The precession around $\vec{M}$ is the electron analog to the Faraday rotation observed with linearly polarized light. It is a quantity that does not depend on A but is caused by the phase difference that develops between majority- and minority-spin wave functions due to the spin dependence of the inner potential. We found that the precession angle ϵ is $16 \pm 2°$ per 1 nm of Co film thickness for an electron energy of 7 eV. It will be discussed in more detail elsewhere.

In conclusion, we note that the very strong spin dependence of the transmission observed in polycrystalline hcp Co opens up the possibility to construct highly efficient spin filters, and to determine the Bohr magneton number n_B of thin films. Furthermore, the precession ϵ around the direction of $\vec{M}$ is unique because it measures the spin dependence of the inner potential otherwise inaccessible. The overall motion of the electron spin observed here is important for the understanding of ultrafast magnetization dynamics. The angles ϕ and ϵ are large considering that, depending on energy, the electrons spend only $\sim 0.3 \times 10^{-15}$ sec per nanometer film thickness within the ferromagnet.

We thank K. Brunner for expert technical assistance and D. Scheiwiller and Professor H. Baltes for helping us with the Si wafers. We are grateful to the Swiss National Science Foundation for having generously supported this project.

[1] U. Bänninger *et al.*, Phys. Rev. Lett. **25**, 585 (1970).
[2] P. W. Anderson, Philos. Mag. **24**, 203 (1971).
[3] S. Doniach, in *Magnetism and Magnetic Materials*, edited by D. C. Graham and J. J. Rhyne, AIP Conf. Proc. No. 5 (AIP, New York, 1971), p. 549.
[4] M. C. Gutzwiler, in *Magnetism and Magnetic Materials*, edited by C. D. Graham and J. J. Rhyne, AIP Conf. Proc. No. 10 (AIP, New York, 1972), p. 1197.
[5] For a review, see L. Kleinman, Comments Solid State Phys. **10**, 29 (1981).
[6] G. Busch *et al.*, Phys. Rev. Lett. **28**, 611 (1972).
[7] J. C. Gröbli *et al.*, Physica (Amsterdam) **204B**, 359 (1995).
[8] H. C. Siegmann, J. Electron Spectrosc. Relat. Phenom. **68**, 505 (1994).
[9] A. Filipe *et al.*, Phys. Rev. Lett. **80**, 2425 (1998), and references therein.
[10] J. Hohlfeld *et al.*, Phys. Rev. Lett. **78**, 4861 (1997).
[11] M. Aeschlimann *et al.*, Phys. Rev. Lett. **79**, 5158 (1997).
[12] A. Scholl *et al.*, Phys. Rev. Lett. **79**, 5146 (1997).
[13] Ganping Ju *et al.*, Phys. Rev. B **57**, R700 (1998).
[14] H. J. Drouhin *et al.*, J. Appl. Phys. **79**, 4734 (1996).
[15] O. Paul, Dissertation ETH Zurich No. 9210, 1990.
[16] H. C. Siegmann, *Selected Topics on Electron Physics*, edited by M. Campbell and H. Kleinpoppen (Plenum, New York, 1996).
[17] M. P. Gokhale and D. L. Mills, Phys. Rev. Lett. **66**, 2251 (1991), and references therein.
[18] J. Glazer and E. Tosatti, Solid State Commun. **52**, 905 (1984).
[19] J. Kirschner, D. Rebenstorff, and H. Ibach, Phys. Rev. Lett. **53**, 698 (1984).
[20] H. Hopster, R. Raue, and R. Clauberg, Phys. Rev. Lett. **53**, 695 (1984).
[21] J. Kirschner, *Polarized Electrons at Surfaces*, Springer Tracts in Modern Physics Vol. 106 (Springer-Verlag, Berlin, 1985), p. 60.